Articles

Novel Tool for Characterization of Noncrystalline Regions in Cellulose: A FTIR Deuteration Monitoring and Generalized Two-Dimensional Correlation Spectroscopy

Yukako Hishikawa,[†] Shun-ichi Inoue,[‡] Jun Magoshi,[§] and Tetsuo Kondo*[,||]

Forestry and Forest Products Research Institute (FFPRI), 1, Matsunosato, Tsukuba, Ibaraki 305-8687, Japan, Nanoarchitectonics Research Center, National Institute of Advanced Industrial Science and Technology (AIST), 1-1-1, Higashi, Tsukuba, Ibaraki 305-8565, Japan, National Institute of Agrobiological Science (NIAS), 1-2-1, Kannondai, Tsukuba, Ibaraki 305-8602, Japan, and Bio-Architecture Center & Graduate School of Bioresource and Bioenvironmental Sciences, Kyushu University, 6-10-1, Hakozaki, Higashi-ku, Fukuoka 812-8581, Japan

Received January 17, 2005; Revised Manuscript Received May 19, 2005

Our previous results indicated that noncrystalline regions in a regenerated cellulose film comprised at least three domains engaged in different manners of molecular assembly [Kondo et al. In *Cellulose Derivatives*; Heinze, T. J., Glasser, W. G., Eds.; ACS Symposium Series 688; American Chemical Society: Washington, DC, 1998; Chapter 12].[1] In this article, we attempt to characterize each of the three noncrystalline domains in the film. The method used was a FTIR monitoring of deuteration from hydroxyl (OH) groups to OD, leading to the two-dimensional (2D) correlation analysis. The time-scan spectra in the OH−OD exchanging reaction were transformed into two kinds of 2D correlation spectra, the synchronous and the asynchronous spectra. Of the two, some cross-peaks were found in the latter spectrum. This suggests that the asynchronous 2D correlation spectrum could differentiate the contribution of OH groups due to different frequencies of hydrogen bonds in each domain. Here we will show the validity of this 2D correlation method as a powerful tool to predict hydrogen-bonding networks of the noncrystalline domains in cellulose.

Introduction

In our previous paper, we investigated the molecular association of β-1,4-glucan chains in noncrystalline regions of cellulose. The combined method of vapor-phase deuteration and Fourier transform infrared (FTIR) spectroscopy followed by a subsequent kinetic analysis of the reaction rates[1,2] was allowed as a powerful tool to understand noncrystalline states of cellulose films. The results indicated that molecular chains in noncrystalline regions were not associated in a random manner but comprised at least three domains with different manners of the molecular association.

The generalized two-dimensional (2D) correlation spectroscopy proposed by Noda[3,4] allows several analyses to expand the usage; for instance, the secondary structure of proteins,[5−9] the premelting behavior of bacterially synthesized polyester,[10] and the temperature-dependent changes in the hydrogen bonds of cotton fibers.[11] The method is applicable to a variety of vibration spectroscopy such as FTIR, near-infrared spectroscopy, and Raman spectroscopy. As the generalized 2D correlation spectroscopy can provide a higher spectral resolution of overlapped absorption bands than one-dimensional spectroscopy, the very minute changes of the system due to the external perturbation are accentuated.

In this paper, we have attempted to characterize each noncrystalline domain above-mentioned in detail and to understand the molecular assembly using the generalization of the 2D correlation spectroscopy. Then, the exchanging reaction of the hydroxyl (OH) groups into OD groups in the noncrystalline regions with time course was supposed as an external perturbation. This generalized 2D correlation spectroscopy was expected to clarify slight differences of the intensity in the overlapped OH bands in the noncrystalline domains. The thus obtained information could lead to a better understanding of hydrogen bonding profiles in noncrystalline and amorphous regions of cellulose films. It should be noted that we want to introduce this novel tool for the characterization of noncrystalline cellulose for those working to produce and better utilize cellulose and cellulose products in industries as well as those in the scientific community.

Experimental Section

Preparation of Noncrystalline Cellulose Films. Noncrystalline cellulose films were prepared by casting of dimethylacetamide/lithium chloride (DMAc/LiCl) cellulose

* To whom correspondence should be addressed. E-mail: tekondo@agr.kyushu-u.ac.jp.
[†] FFPRI.
[‡] AIST.
[§] NIAS.
[||] Kyushu University.

10.1021/bm050032k CCC: $30.25
Published on Web 07/08/2005

solution in the same way as reported previously.[2] The films with 5 μm in thickness exhibited a relative crystallinity index (Cr.I.) of 0.0%, determined by X-ray analysis. It was then dried thoroughly in a vacuum oven at 50 °C in order to remove all residual water prior to deuteration. In general, a cast cellulose film prepared in this way is believed to be "amorphous", that is a state having no preferable order.

Deuteration and FTIR Measurements. The noncrystalline cellulose film was deuterated in a special homemade sample cell for monitoring IR absorption of OH groups in the deuteration process as reported previously.[2] The film was sealed in the cell against an access of air during the vapor-phase deuteration. FTIR spectra were recorded at the desired intervals using a Nicolet Magna-IR 550 spectrometer. The parameters for the IR measurements were as follows: 6 scans with a 2 cm^{-1} resolution (scanning time was 69 s), a DTGS detector, and the wavenumber region investigated ranged from 4000 to 400 cm^{-1}. Spectra were recorded continuously until the OH−OD exchange reaction reached an equilibrium state.

Generalized 2D Correlation Spectroscopy. *Calculations.* Generalization of 2D correlation spectra was carried out using the formulas according to Noda.[3] During vapor-phase deuteration as an external perturbation, the spectral intensity was changed with time course. A set of such time-domain spectral intensities called dynamic spectral intensity ($\tilde{y}(\nu, t)$) was Fourier transformed into the frequency domain (ω) spectra, using the following equation:

$$\tilde{Y}_1(\omega) = \int_{-\infty}^{\infty} \tilde{y}(\nu_1, t) e^{-i\omega t}\, dt = \tilde{Y}_1^{Re}(\omega) + i\tilde{Y}_1^{Im}(\omega)$$

and

$$\tilde{Y}_2^*(\omega) = \int_{-\infty}^{\infty} \tilde{y}(\nu_2, t) e^{+i\omega t}\, dt = \tilde{Y}_2^{Re}(\omega) - i\tilde{Y}_2^{Im}(\omega)$$

where $\tilde{Y}_1(\omega)$ and $\tilde{Y}_2^*(\omega)$ are the Fourier transformed time-domain dynamic spectral intensities of $\tilde{y}_1(\nu_1, t)$ and $\tilde{y}_2(\nu_2, t)$ which are observed at corresponding ν_1 and ν_2, spectral variables chosen arbitrarily. t is time, and $\tilde{Y}_1(\omega)^{Re}$ and $\tilde{Y}_2(\omega)^{Re}$ are the real parts, whereas $\tilde{Y}_1(\omega)^{Im}$ and $\tilde{Y}_2(\omega)^{Im}$ are the imaginary parts of each complex Fourier transform of the time-domain dynamic spectral intensity.

The complex 2D correlation intensity is defined as

$$\Phi(\nu_1, \nu_2) + i\Psi(\nu_1, \nu_2) = \frac{1}{\pi T}\int_0^{\infty} \tilde{Y}_1(\omega)\cdot\tilde{Y}_2^*(\omega)\, d\omega$$

where T is a period of time. The real and imaginary parts of the complex 2D correlation intensities, ($\Phi(\nu_1, \nu_2)$) and ($\Psi(\nu_1, \nu_2)$) are referred as a synchronous correlation spectrum and an asynchronous correlation spectrum, respectively. The former indicates the relatively large changes and the overall similarity of the time-domain behavior of spectral intensity[3] measured at two separate wavenumbers. The latter represents minor changes generally. Cross-peaks in the asynchronous spectrum map appear when the spectral intensities at wavenumbers ν_1 and ν_2 vary out of phase with each other.[3]

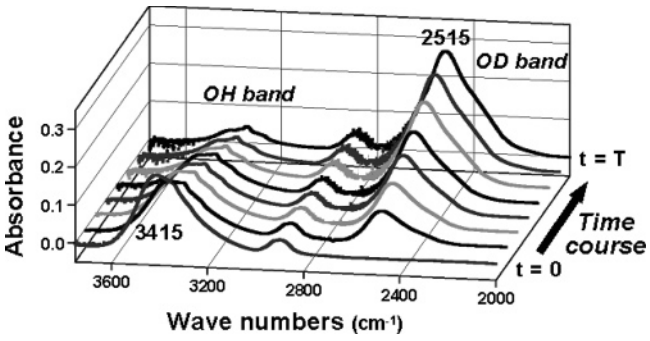

Figure 1. Changes in OH and OD IR absorption bands in one-dimensional spectra with the elapsed time during the vapor-phase deuteration process for the noncrystalline regenerated cellulose film (crystallinity index: Cr.I. = 0.0%); t is the deuteration time and T is the maximum value of the deuteration time.

The range of wavenumbers for the calculations was set from 3700 to 3000 cm^{-1}, which represents the OH bands due to stretching vibration in anhydroglucose units of cellulose.[12] All calculations were made using IGOR Pro 3.14 (WaveMetrics Inc.) as a Windows software.

Furthermore, it should be added that the Hilbert transform algorithm was also proposed recently to facilitate the calculation process of 2D correlation spectra,[13,14] but both of ours and the calculation algorithm are supposed to provide the same results.

Results and Discussion

(i) Kinetic Analysis of Deuteration Process, Leading to the Analysis by Generalized 2D Correlation Spectroscopy. We had proposed a model of the supermolecular structure in amorphous and noncrystalline regions of cellulose.[15] It was mentioned that the aggregated molecular states in the noncrystalline film were not homogeneous,[15] similarly to the result on the deuteration of the same film.[2] Therefore, both of the two results indicated the presence of the heterogeneity in aggregation, which may mostly influence the deuteration rate. Thus, our previous article[2] attempted to at first examine indirect structural information on how cellulose molecules in the regions are associated or packed using exchanging rates in the deuteration process of the OH groups. This analysis was actually based on the hypothesis that the simple H−D exchanging rate from OH to OD may be too fast to exhibit significant differences, as long as D_2O could approach close enough to OH. Namely, as the replacing rate is fast enough to be negligible, the diffusing deuteration rate in the film may be the major factor to determine the final reaction rate. Thus, the rate itself could possibly indicate the state of the molecular packing or association.

Figure 1 summarizes retraced results of our previous study in changes of OH and OD bands in one-dimensional IR spectra for the noncrystalline cellulose film during a vapor-phase deuteration process. Although the intensity of the OH absorption band at 3415 cm^{-1} decreased during the deuteration, the absorption band at 2515 cm^{-1} due to a stretching vibration mode of OD groups appeared and increased with progress of the deuteration. In the equilibrium state of the deuteration, the absorption bands due to OH groups at 3340 cm^{-1} still remain. These remaining OH absorption bands

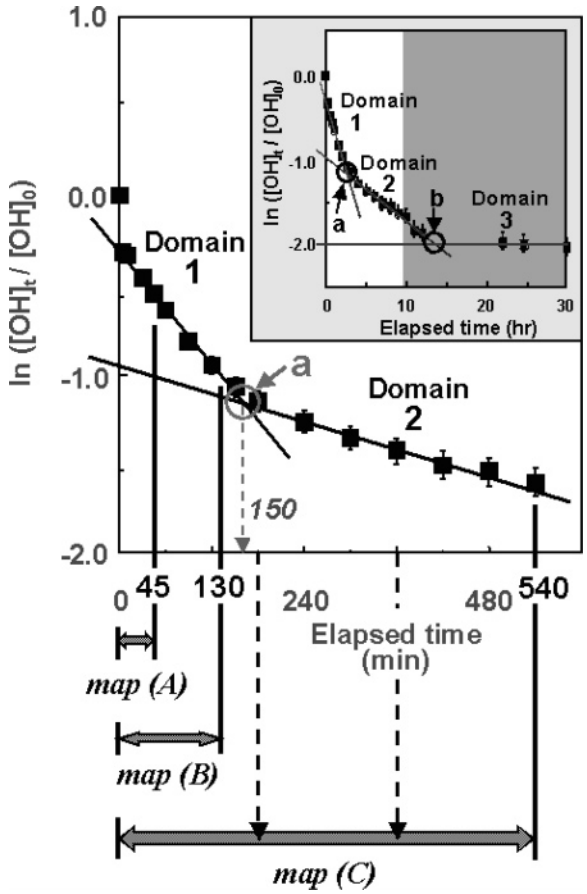

Figure 2. Relationship between the logarithmic ratio of decreasing concentration in OH groups, $\ln\{[OH]_t/[OH]_0\}$, with time (t) ranged from 0 to 540 min in the deuteration process for the noncrystalline regenerated cellulose film. The three time ranges from map A to C were employed for synchronous and asynchronous 2D correlation spectra maps. In the inserted figure indicating the entire process (elapsed time in hours), the three solid lines on the plot represent a calculated regressed fit of the points. The kinetic behavior was separated into three distinct single reactions.

indicated the presence of intact OH groups in the noncrystalline regions as mentioned in our previous report.[2]

Then, the kinetic analysis was carried out in the previous paper on the reduction of the OH bands. The OH−OD exchange reaction was considered as pseudo-first-order kinetics because of the excess amount of deuterium oxide (D_2O) molecules penetrating in the noncrystalline (or amorphous) film. In fact, the plot of the logarithm of the decreasing ratio of OH groups, $\ln\{[OH]_t/[OH]_0\}$, versus the time (t) during the deuteration process did not exhibit a linear relationship. Thus, the relationship was reasonably hypothesized to contain three distinct single reactions with different rate constants as shown in the inserted figure of Figure 2. This means that some domains may be distributed in the noncrystalline regions of the film. Namely, as our previous article[2] did, it was suggested that assembly states of molecular chains in noncrystalline regions were not necessarily homogeneous but organized to some extent to form three domains.

In this study, each domain is coded according to the magnitude of the rate constant. For example, as reaction 1 in Figure 2 had the highest rate constant, the corresponding molecular organizing domain is coded as domain 1. The higher rate constant indicates that the D_2O penetrated the domain more easily. In other words, molecular chains may be assembled more loosely in the domain, providing a higher exchanging rate of OH into OD. In this way, the molecular chains in domain 2 were to be packed more tightly than those in domain 1. As domain 3 had more intact OH groups, it was indicated that molecular chains were packed the most sturdily of the three domains.

The intersection between the extrapolated straight lines as shown in the arrows a and b of the insert in Figure 2 indicates the elapsed time for completion of the deuteration of OH groups in domains 1 and 2, respectively. The deuteration of the two domains, 1 and 2, was ended after 2.5 and 13.5 h, respectively. As stated above, OH groups in domain 3 were mostly undeuterated. The relative ratio of the OH presence in each domain to the total ones including OH groups on the surface was also estimated using the value at the y ordinate obtained by extrapolation of the straight lines as shown in the same figure. The value by the line of the highest slope corresponds to a sum of the relative ratio of the OH groups in all domains 1, 2, and 3. Similarly, the value by the straight line of the lower (second) slope provides the relative ratio of the OH groups in both domains 2 and 3. Further, the value given by the straight line of the lowest slope (third) represents the relative ratio of the OH groups only in domain 3. Thus, the relative ratio of the OH groups in each domain should be given by the subtraction among the above three relative ratios. The relative ratio obtained in this way was 40.8%, 17.7%, and 13.3% in domains 1, 2, and 3, respectively. The rest of the OH groups, 28.2%, could not be involved in these domains but on the surface of the film.

As the value of the rate constant in domain 1 was the highest of the three, exchange of OH groups into OD groups within 45 min (map A of Figure 2) may occur mostly in domain 1 where the molecular packing is considered most loosened. Since OH groups in both domains 1 and 2 were competitively deuterated during the time in the range of map B, the change of the rate constant could also reflect the situation of hydrogen bonds resulting in the molecular packing in both domains. In the third period in map C, the rate constant reflected the situation in domain 2. By this period, deuteration of OH groups in domain 1 may be mostly completed, which means that hydrogen bonds involved only in domain 2 may be revealed in map C. As for domain 3, no rate constant was obtained, which was attributed to large amounts of unexchangeable OH groups into OD groups in the domain.

(ii) 2D Correlation Spectra. Three kinds of synchronous and asynchronous 2D correlation spectra were also obtained based on the deuteration elapsed time shown in Figure 2 using formulas described in the Experimental Section. In general, a synchronous 2D correlation spectrum represents the large changes, and moreover, the simultaneous or coincidental changes of spectral intensities.[3] The spectrum is symmetric regarding the diagonal of the plane map produced by two independent wavenumbers. Usually, two kinds of correlation peaks are supposed to be observed in the map. Autopeaks appear on the diagonal only in the

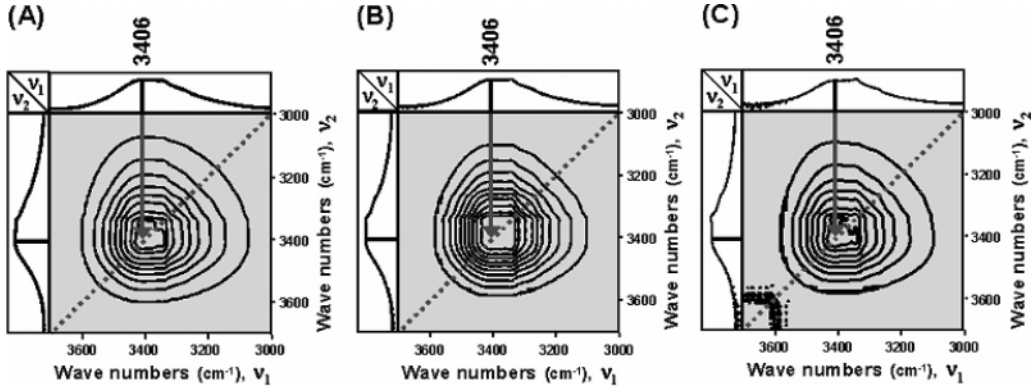

Figure 3. Synchronous 2D correlation spectra plotted as contour maps according to the elapsed time of the vapor-phase deuteration of the noncrystalline regenerated cellulose film: (A) the time range from 0 to 45 min, (B) the time range from 0 to 130 min, and (C) the time range from 0 to 9 h, respectively.

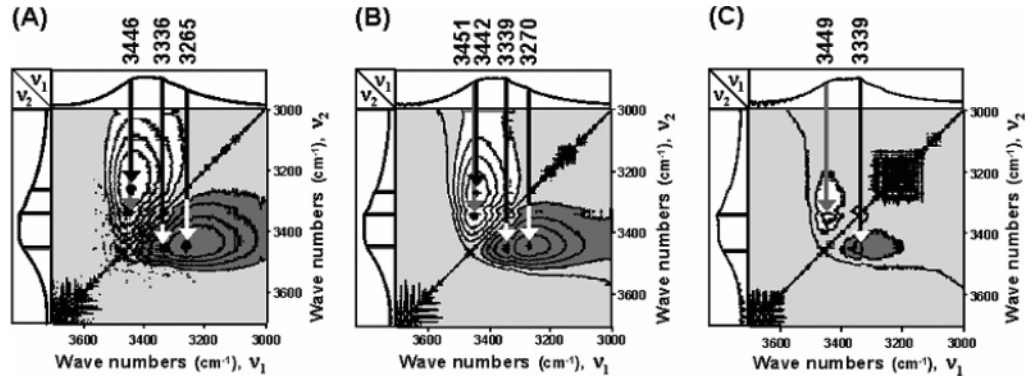

Figure 4. Asynchronous 2D correlation spectra plotted as contour maps according to the elapsed time of the vapor-phase deuteration of the noncrystalline regenerated cellulose film: (A) the time range from 0 to 45 min, (B) the time range from 0 to 130 min, and (C) the time range from 0 to 9 h, respectively.

synchronous spectrum map, and they represent the changes associated with the peak position.[16] The other peaks called cross-peaks are located at off-diagonal positions, and those in the synchronous spectrum are developed when two different IR spectral signals associated with molecular vibrations from the different functional groups respond to the perturbation simultaneously.[6] In the present study, the individual synchronous 2D correlation spectra depending on the three kinds of elapsed periods of the deuteration for domain 1 and 2 were plotted as contour maps as shown in maps A−C of Figure 3. Map A indicates a correlation spectrum at the deuteration time range 0 to 45 min, map B refers to that at the time range 0−130 min, and similarly a correlation spectrum ranging from 0 to 9 h is shown in the map C. Each map has only one autopeak at 3406 cm^{-1} and no cross-peak. For this, there are two possible reasons in the following: The appearance of one strong autopeak indicates that the change in intensity was too large during the exchanging process in each range of the elapsed time, and thus the rest of features including cross-peaks in the map became obscured. The other possible reason is that there were no simultaneous changes of the correlated spectral intensities, which may differentiate OH groups belonging to different domains with each other.

In addition to the synchronous spectra, asynchronous 2D correlation spectra were required to investigate details of the phenomenon, since the cross-peaks in the asynchronous spectrum map indicate that absorption bands are dependent on the sources or functional groups in different molecular environments.[3] Thus, an asynchronous 2D correlation spectrum is supposed to reveal the minor changes. In general, the spectrum is antisymmetric across the diagonal of the plane map and there are not autopeaks but cross-peaks at off-diagonal positions in the map. Cross-peaks in the asynchronous spectrum map can grow when the spectral intensities at wavenumbers of ν_1 and ν_2 are varied out of phase with each other.[4] In other words, cross-peaks usually suggest chemical interactions between the functional groups that are decoupled and uncoordinated.[6] Therefore, the asynchronous 2D correlation spectra can be used to deconvolute the overlapped bands in different molecular environments, as stated above. Figure 4 shows contour maps of the three individual asynchronous 2D correlation spectra depending on the increasing elapsed time (maps A−C) in the deuteration that are separated by the same deuteration time range used for the synchronous 2D correlation. The appearance of cross-peaks in each map suggested the existence of OH groups in different molecular environments. In map A of Figure 4, the two distinguished cross-peaks appeared at wavenumbers of 3446 and 3265 cm^{-1}, although another slight indication of 3446 and 3336 cm^{-1} may have been seen. The major cross-peaks may represent the large contribution of hydrogen bonds that are in variety of the status. As to regenerated cellulose, OH absorption bands appearing at higher wavenumbers than 3400 cm^{-1} are classified as a reflection of intramolecular hydrogen bonds,[12] whereas OH bands at lower wavenumbers than 3400 cm^{-1} are grouped into contribution of intermolecular hydrogen bonds. There-

Table 1. Comparison of Wave Numbers in Individual Map Obtained by Asynchronous 2D Correlation Spectroscopy

		wave numbers (cm^{-1})		
	map	major peak		minor peak
intramolecular	A	3446		3446
hydrogen bonds	B	3442	3451	
	C		3449	
intermolecular	A	3265		3336
hydrogen bonds	B	3270	3339	
	C		3339	
domain		1	2	

fore in the asynchronous 2D correlation in this study, the absorption band at 3446 cm^{-1} may be derived from intramolecular hydrogen bonds, whereas the absorption band at 3265 cm^{-1} appeared due to intermolecular hydrogen bonds. The map B period of Figure 4 provided four major cross-peaks attributed to two intramolecular hydrogen bonds at wavenumbers of 3451 and 3442 cm^{-1} and two intermolecular hydrogen bonds at 3339 and 3270 cm^{-1}, respectively. There were also the two distinguished cross-peaks in map C at 3449 and 3339 cm^{-1} although this case had also the similar trend of the case of map A which may have the slight indication. The former may be arisen from intramolecular hydrogen bonds and the latter may be derived from intermolecular hydrogen bonds.

(iii) Characterization of Hydrogen Bonding. The wavenumbers due to both intra- and intermolecular hydrogen bonds provided from the three maps in Figure 4 were listed and compared in Table 1. As stated before, the map B period includes the deuteration processes in the domains 1 and 2, because of the competitive deuteration depending on packing states of the two domains. Therefore, the four distinct cross-peaks were possibly obtained. They are considered to be due to two couples of intra- and intermolecular hydrogen bonds. Of the two, a couple of wavenumbers of 3451 and 3339 cm^{-1} due to intra- and intermolecular hydrogen bonds, respectively, were similar to those obtained in map C. Here, map C is considered to provide information on domain 2 since the map C period is supposed to be passed after completion of the deuteration process in domain 1. Therefore, the wavenumbers obtained in map B may be overlapped with those due to OH groups in domain 2 that were derived from map C. Moreover, a couple of wavenumbers of 3446 and 3336 cm^{-1} obtained from the minor cross-peak in map A were also similar to the obtained wavenumbers in maps B and C. Though map A suggests predominantly domain 1 as stated above, the wavenumbers obtained in map A may also refer to OH groups in domain 2 because OH groups in both domains 1 and 2 were deuterated competitively. The rest of the wavenumbers in map B were a couple of 3442 and 3270 cm^{-1} attributed to intra- and intermolecular hydrogen bonds, respectively. The frequencies were fairly close to the wavenumbers of the major peaks obtained in map A. Since map A reflects mainly the loosened packed domain 1, OH groups are supposed to be deuterated most rapidly, and thereby, the present hydrogen bonds are assumed to correspond to those in the domain 1.

The force constants of OH groups forming the intra- and intermolecular hydrogen bonding in domains 1 and 2 were also calculated using the obtained wavenumbers. The equation used was stated below. It is assumed that the OH group was a diatomic molecule, and the bond between the two nuclei of O and H behaves as a spring, in other words, the harmonic oscillator that obeys Hooke's law. By the quantum mechanical treatment of the harmonic oscillator, the molecule can have only discrete vibrational energy levels characterized by the quantum numbers $\nu = 0, 1, 2, 3$, etc. The vibrational spectra of diatomic molecules usually represent excitation from the $\nu = 0$ to the $\nu = 1$ energy levels. This excitation provides the energy eigenvalue ΔE

$$\Delta E \text{ (in joules)} = \text{wavenumbers } (cm^{-1})\ h \text{ (Js)}\ c \text{ (m/s)}\ 100 \text{ (cm/m)} = h\,(k/\mu)^{1/2}/2\pi$$

where h is Planck's constant, c is the velocity of light in vacuum, k is the force constant (N/m), and μ stands for $m_1m_2/(m_1 + m_2)$, where m_1 and m_2 are masses (kg) of the two nuclei, O and H, respectively.[17]

The force constants of OH groups in domain 1 thus calculated were 664 and 596 N/m corresponding to the intra- and intermolecular hydrogen bond, respectively. As to domain 2, the corresponding constants were 665 and 623 N/m. The magnitude of the force constants represents the strength of the bond between O and H atoms. By comparison of the magnitude of those constants, OH groups in the domain 1 that have weaker bonding strength between O and H atoms are considered more facile to be exchanged than those in the domain 2. Thus, the major contribution due to hydrogen bonds in each domain can be detected.

Tashiro, et al. calculated the force constants of the O−H- - -O forming hydrogen bonds in the crystalline regions of both native cellulose and regenerated cellulose.[18] In fact, the force constants of OH groups engaging intermolecular hydrogen bonds in both crystalline forms were reasonably quite different from our results for noncrystalline regions of regenerated cellulose. This result indicates that intermolecular hydrogen bonds alter by a variety of the molecular association of cellulose in a changing process of the status in cellulose from the noncrystalline to the crystalline phases.

Conclusion

This article attempted to introduce a new tool to investigate noncrystalline regions in cellulose films, which is of importance to understand structure−property relationship in cellulosic materials.

In our previous report, the combination of vapor-phase deuteration and one-dimensional FTIR measurements followed by a subsequent kinetic analysis on the noncrystalline regions of the regenerated cellulose film clarified presence of three domains (domains 1, 2, and 3) having a different molecular packing that were distributed, even though the conventional X-ray diffraction patterns exhibited were amorphous. In this study, the combined method with generalized 2D correlation spectroscopy was applied to

investigate more details of such super- and supramolecular structures of noncrystalline domains. Of the two kinds of 2D correlation spectroscopy, the asynchronous 2D correlation spectroscopy made it possible to differentiate wavenumbers due to intra- and intermolecular hydrogen bonds in both domains 1 and 2. In addition, the force constants of OH groups influenced by the hydrogen bonds were calculated. The result indicated that OH groups in the domain 1 possessed a weaker bonding strength between O and H atoms, which are considered more facile than those in domain 2 to exchange O−H into O−D under a D_2O vapor atmosphere. Thus, the major contribution due to hydrogen bonds in each domain can be detected although they have a variety of bonding modes. Furthermore, the force constants of OH groups engaged in intermolecular hydrogen bonds of the noncrystalline domains were found to be different when compared with those in the crystalline forms reported previously. This may be attributed to the difference in states of the molecular assembly between the noncrystalline and the crystalline phases.

In this way, the method presented in this study has proved to be a powerful tool to characterize noncrystalline domains including hydrogen bonds. Furthermore, this method could be applied to characterize other molecular assembling states such as cross-linking of hydrogels and structures of micelles in the related carbohydrate polymers as well as cellulose that have been so far difficult to characterize.

Acknowledgment. The authors thank Core Research for Evolutional Science and Technology (CREST) programs supported by Japan Science and Technology Corporation (JST), and a Grant-in-Aid for Exploratory Research (No. 14656071) by Ministry of Education, Culture, Sports, Science and Technology (MEXT). This research was also supported in part by a Grant-in-Aid for Scientific Research (No. 14360101), Japan Society for the Promotion of Science (JSPS).

References and Notes

(1) Kondo, T.; Kataoka, Y.; Hishikawa, Y. In *Cellulose Derivatives*; Heinze, T. J.; Glasser, W. G., Eds.; ACS Symposium Series 688; American Chemical Society: Washington, DC, 1998; Chapter 12.
(2) Hishikawa, Y.; Togawa, E.; Kataoka, Y.; Kondo, T. *Polymer* **1999**, *40*, 7117−7124.
(3) Noda, I. *Appl. Spectrosc*. **1993**, *47*, 1329−1336.
(4) Noda, I.; Dowrey, A. E.; Marcott, C.; Story, G. M.; Ozaki, Y. *Appl. Spectrosc*. **2000**, *54*, 236A-248A.
(5) Nabet, A.; Pezolet. M. *Appl. Spectrosc*. **1997**, *51*, 466−469.
(6) Sefara, N. L.; Magtoto, N. P.; Richardson, H. H. *Appl. Spectrosc*. **1997**, *51*, 536−540.
(7) Meskers, S.; Ruysschaert, J.-M.; Goormaghtigh, E. *J. Am. Chem. Soc*. **1999**, *121*, 5115−5122.
(8) Dzwolak, W.; Kato, M.; Shimizu, A.; Taniguchi, Y. *Appl. Spectrosc*. **2000**, *54*, 963−967.
(9) Robert, P.; Mangavel, C.; Renard, D. *Appl. Spectrosc*. **2001**, *55*, 781−787.
(10) Wu, Q.; Tian, G.; Sun, S.; Noda, I.; Chen, G.-Q. *J. Appl. Polym. Sci*. **2001**, *82*, 934−940.
(11) Kokot, S.; Czarnik-Matusewicz, B.; Ozaki, Y. *Biopolymers* **2002**, *67*, 456−469.
(12) Marchessault, R. H.; Liang, C. Y. *J. Polym. Sci*. **1960**, *43*, 71−84.
(13) Noda, I. *Appl. Spectrosc*. **2000**, *54*, 994−999.
(14) Noda, I. *Vib. Spectrosc*. **2004**, *36*, 143−165.
(15) Kondo, T.; Sawatari, C. *Polymer* **1996**, *37*, 393−399.
(16) Ekgasit, S.; Ishida, H. *Appl. Spectrosc*. **1995**, *49*, 1243−1253.
(17) Harris, D. C.; Bertolucci, M. D. *Symmetry and Spectroscopy*, *An Introduction to Vibrational and Electronic Spectroscopy*; Dover Publications: New York, 1989; pp 100-105.
(18) Tashiro, K.; Kobayashi, M. *Polymer* **1991**, *32*, 1516−1526.

BM050032K